

Effects of Exosomes Derived from Kidney Tubular Cells on Diabetic Nephropathy in Rats

Fereshtesadat Fakhredini, Ph.D.^{1,2}, Esrafil Mansouri, Ph.D.^{1,2}, Seyyed Ali Mard, Ph.D.³, Armita Valizadeh Gorji, Ph.D.⁴, Mohammad Rashno, Ph.D.⁵, Mahmoud Orazizadeh, Ph.D.^{1,2*}

1. Cell and Molecular Research Centre, Faculty of Medicine, Ahvaz Jundishapur University of Medical Sciences, Ahvaz, Iran
2. Department of Anatomical Sciences, Faculty of Medicine, Ahvaz Jundishapur University of Medical Sciences, Ahvaz, Iran
3. Department of Physiology, Physiology Research Centre, Research Institute for Infectious Diseases of the Digestive System, School of Medicine, Ahvaz Jundishapur University of Medical Sciences, Ahvaz, Iran
4. Department of Bone Marrow Transplantation, Ahvaz Jundishapur University of Medical Sciences, Ahvaz, Iran
5. Department of Immunology, Faculty of Medicine, Ahvaz Jundishapur University of Medical Sciences, Ahvaz, Iran

*Corresponding Address: P.O.Box: 61335, Department of Anatomical Sciences, Faculty of Medicine, Ahvaz Jundishapur University of Medical Sciences, Ahvaz, Iran
Email: orazizadehm@gmail.com

Received: 25/April/2020, Accepted: 16/August/2020

Abstract

Objective: One of the severe complications and well-known sources of end stage renal disease (ESRD) from diabetes mellitus is diabetic nephropathy (DN). Exosomes secreted from diverse cells are one of the novel encouraging therapies for chronic renal injuries. In this study, we assess whether extracted exosomes from kidney tubular cells (KTCs) could prevent early stage DN *in vivo*.

Materials and Methods: In this experimental, exosomes from conditioned medium of rabbit KTCs (RK13) were purified by ultracentrifuge procedures. The exosomes were assessed in terms of morphology and size, and particular biomarkers were evaluated by transmission electron microscopy (TEM), scanning electron microscopy (SEM), Western blot, atomic force microscopy (AFM) and Zetasizer Nano analysis. The rats were divided into four groups: DN, control, DN treated with exosomes and sham. First, diabetes was induced in the rats by intraperitoneal (i.p.) administration of streptozotocin (STZ, 50 mg/kg body weight). Then, the exosomes were injected each week into their tail vein for six weeks. We measured 24-hour urine protein, blood urea nitrogen (BUN), and serum creatinine (Scr) levels with detection kits. The histopathological effects of the exosomes on kidneys were evaluated by periodic acid-Schiff (PAS) staining and expressions of miRNA-29a and miRNA-377 by quantitative real-time polymerase chain reaction (qRT-PCR).

Results: The KTC-Exos were approximately 50-150 nm and had a spherical morphology. They expressed the CD9 and CD63 specific markers. Intravenous injections of KTC-Exos potentially reduced urine volume ($P<0.0001$), and 24-hour protein ($P<0.01$), BUN ($P<0.001$) and Scr ($P<0.0001$) levels. There was a decrease in miRNA-377 ($P<0.01$) and increase in miRNA-29a ($P<0.001$) in the diabetic rats. KTC-Exos ameliorated the renal histopathology with regulatory changes in microRNAs (miRNA) expressions.

Conclusion: KTC-Exos plays a role in attenuation of kidney injury from diabetes by regulating the miRNAs associated with DN.

Keywords: Diabetic Nephropathy, Exosomes, Kidney, miRNAs

Cell Journal (Yakhteh), Vol 24, No 1, January 2022, Pages: 28-35

Citation: Fakhredini FS, Mansouri E, Mard SA, Valizadeh Gorji A, Rashno M, Orazizadeh M. Effects of exosomes derived from kidney tubular cells on diabetic nephropathy in rats. Cell J. 2022; 24(1): 28-35. doi: 10.22074/cellj.2022.7591.
This open-access article has been published under the terms of the Creative Commons Attribution Non-Commercial 3.0 (CC BY-NC 3.0).

Introduction

It is widely accepted that diabetic nephropathy (DN) is one of the destructive complications of diabetes mellitus and one of the main causes of End-stage renal disease (ESRD) worldwide (1). Statistically, approximately 347 million people suffer from diabetes, and this number is estimated to reach 430 million in 2030. DN is becoming more common and has almost reached epidemic proportions (1, 2). The diverse structural and functional modifications responsible for DN pathogenesis include hemodynamic changes, expression or activation of different proteins and signalling pathways, oxidative stress, mesangial cell expansion, fibrosis development and glomerulosclerosis (GS) (3). Despite common treatments that include ameliorating high blood

pressure and hyperglycaemia, there are no efficient treatment options that counteract and reverse DN (4-6). Over the past decade, cell therapy is increasingly considered to be one of the newly developed regenerative therapies for renal damages (7).

The results of studies show that the effectiveness of treatment on these cells is strongly associated with exosomes, which are membrane-bound extracellular vesicles (8). Exosomes are microvesicles that have a two-layer lipid membrane and are secreted by different cell types. They play an important role as an alternative mechanism for biological transport between distant cells. This transport is characterised by an intracellular packaging process in which various proteins and other gene products are loaded into exosomal carriers and then released into the extracellular environment (9). The two lipid layers of the exosomes protect their contents from destruction

by proteases and nucleases present in the bloodstream. Exosomes also have protein markers on their surface that reflect their endosomal origin. They are considered to be cell-derived vesicles, 30 to 100 nm in diameter, which are discharged into the microenvironment via numerous cell types (10). Exosomes consist of microRNAs (miRNAs), proteins, and mRNAs that can be transferred to target cells and cause epigenetic and genetic changes to the target cells (11). Horizontal transfer of vesicular miRNAs and mRNAs may result in an angiogenic program in endothelial cells or modulate the injured cell phenotypes (12).

Based on the results of studies, miRNAs are considered to be one of the groups of non coding RNAs that are expressed in all tissues. They play important roles in various diseases, including diabetes (13). Increased glucose levels stimulate *miR-377* expression, which results in increased fibronectin production via repression of superoxide dismutase and p21-activated kinase (14). *miR-377* targets hemeoxygenase-1 (HO-1) and HO-1 prevents DN through antioxidant effects. The *miR377/HO-1* pathway could be a new pathway where *miR-377* stimulates DN via HO-1 (15, 16). Three members of the *miR-29* family are suppressed under elevated glucose conditions in proximal tubular cells, mesangial cells and podocytes (17). The members of the *miR-29* family are responsible for anti-fibrotic effects in DN. *miR-29a* directly targets the 3'UTR of *COL4a1* and *COL4a2*, and leads to decreased expressions of these two fibrotic genes (18, 19).

The current study aims to evaluate the effects of exosomes derived from kidney tubular cells (KTCs) on DN in a rat model of diabetes. We propose that KTC-Exos could modulate kidney complications from diabetes and they could be a possible new regulator in DN therapy.

Materials and Methods

In this experimental study, male Sprague-Dawley rats (n=40, 220-270 g) were obtained from the Animal House Centre of Ahvaz Jundishapur University of the Medical Sciences (Ahvaz, Iran). The rats were kept in cages on a 12/12-hour light/dark cycle at 21-24°C. Ethical Committee of Ahvaz Jundishapur University of Medical Sciences approved this study (IR.AJUMS.ABHC.REC.1398.008).

Culture of the kidney tubular cell line

The rabbit KTC line (RK13, NCBI code: C523) was purchased from Pasteur Institute of Iran and immediately transferred to Dulbecco's Modified Eagle Medium (DMEM) high glucose (Gibco, UK) that consisted of 2 mM L-glutamine and 100U penicillin/streptomycin (all from Invitrogen, Waltham, MA, USA) and 10% fetal bovine serum (FBS, Gibco, UK). The cells were stored in an incubator at 37°C and 5% CO₂ to enable proliferation. The medium was replaced after five days, and the cells were washed with phosphate buffered saline (PBS, Sigma, USA) in order to remove any non-adherent cells.

The cells were passaged using 0.25 % trypsin when they were ~90% confluent.

Isolation and purification of the kidney tubular cell-derived exosomes

KTC-Exos were prepared and treated according previously published protocols (20, 21). Briefly, the 80-90% confluent cells were washed with PBS, and then cultured at 37°C and 5% CO₂ in DMEM without FBS for an additional 48 hours. The exosomes were isolated from the supernatant of passage-2 cells, 48 hours after cultivation in serum-free DMEM. The conditioned medium was collected and centrifuged at 300 g for 10 minutes, 2000 g for 10 minutes, and 10 000 g for 30 minutes at 4°C to remove the cells, large dead cells, and debris. The resultant supernatant was filtered through a sterile 0.22 µm (Millipore, USA) filter to remove any remaining cells and cellular debris. Afterwards, the supernatant was transferred to an ultra-clear tube (Millipore, USA) and centrifuged with a high-speed centrifuge at 60 000×g at 4°C for 90 minutes to isolate the purified exosomes, as a final pellet (22). The KTC-Exos pellet was resuspended in 200µl of PBS and stored at -80°C. The protein contents of the KTCs-Exos solution were determined by the Bradford assay, according to the manufacturer's instructions (Thermo Fisher Scientific, USA). Absorbance was read at 595 nm using a microplate reader.

Transmission electron microscopy and scanning electron microscopy of kidney tubular cell-derived exosomes

Both transmission electron microscopy (TEM) and scanning electron microscopy (SEM) were used to assess the morphological features of the exosomes. First, the exosomal pellet was fixed with 1% glutaraldehyde (Sigma, USA) and then 20 µl of the fixed exosomes were inserted on a carbon-coated grid and allowed to dry at room temperature for 30 minutes. Then, a LEO 906 TEM (Zeiss, Germany) was used to each the samples were washed twice with PBS for 5 minutes, and stained with 1% uranyl acetate for 10 minutes before they were visualized under a TEM at an accelerating voltage of 80 kV. DigitalMicrograph software (Gatan, Inc., Washington, DC, USA) was used to record the TEM images that were acquired with an Orius 200 camera (Gatan, Inc., Washington, DC, USA). We also assessed the particle surface morphology by SEM. A total of 1 to 5 µl of the dried sample was placed on a silicon chip, fixed with 2% paraformaldehyde and sputter-coated with gold-palladium, then visualised by SEM at 30 kV.

Determination of the distribution and size of the kidney tubular cell-derived exosomes by dynamic light scattering, using a Zetasizer Nano device

Dynamic light scattering (DLS) was used to analyse the solvent nanoparticle (NP), which is capable of measuring particles in a solution quickly, easily, and without sample preparation. For this purpose, the extracted exosomes

were resuspended in PBS (100 µl). After shaking the solution, a Malvern Zetasizer Nano device (Malvern Instruments, Malvern, UK) was used to measure the sizes of the exosomes.

Western blot for characterisation of the kidney tubular cell-derived exosomes surface markers

We used Western blotting to characterise the KTC-Exo surface markers. The presence of two specific surface markers, CD9 and CD63, confirmed the KTC-Exos identity (23). Briefly, the exosomes were lysed with RIPA/PI buffer (Santa Cruz Biotechnology, Inc., Dallas, TX, USA) and the level of protein was estimated by the Bradford protein assay. Then, the KTC-Exos protein was loaded onto a 12% sodium dodecyl sulphate/poly-acrylamide gel electrophoresis (SDS-PAGE). In addition, the protein samples were transferred to the polyvinylidenedifluoride membrane via electroblotting the membrane of polyvinylidenedifluoride (Millipore, USA) at 100 mA for 1.5 hours. Then, the membranes were exposed to the primary rabbit polyclonal anti-CD9 and anti-CD63 antibodies, and the β -actin antibody (Abcam, UK) in order to test for the presence of CD63 and CD9. The membranes were washed three times for 5 minutes each time in $1\times$ tris-HCl buffered saline with Tween (TBST) that consisted of TBS and 0.1% Tween 20. Incubation was done in TBST with the horseradish peroxidase-conjugated goat anti-rabbit secondary antibody (Abcam, UK) for one hour. ECL solution was applied for detection and imaging of the proteins in the membrane. Lumigan PS-3 substrate is catalyzed in ECL solution by a horseradish peroxidase enzyme connected to the secondary antibody. The radiation produced by luminol was released as a result of this reaction and was detected using special films. The protein bands that resulted were compared between groups and statistically analyzed.

Assay of KTC-Exos -Exo by atomic force microscopy

The exosomal pellet was prepared over several rounds of high-speed centrifugation, and then diluted in 5 ml of deionized water and vortexed. The exosomal solution was subsequently transferred to the south-central laboratory of Ahvaz Jundishapur University of Medical Sciences. Distribution, size, NP size, characteristics, morphology, and surface features of the soluble exosomes were analysed by atomic force microscopy (AFM). The two-dimensional images were also analysed.

Diabetes induction

The healthy male rats were allowed to fast for 24 hours before diabetes induction. A single intraperitoneal (i.p.) injection of streptozotocin (STZ, 50 mg/kg body weight, Sigma, USA) (24) that was recently dissolved in citrate buffer (0.1 M at pH=4.5) was used to induce diabetes. The control animals were injected with the vehicle buffer. Blood samples were obtained from the animals' tail veins 72 hours after the STZ injection. Fasting blood glucose levels were measured by a glucose strip test and a glucometer (EasyGlucoBlood Glucose Monitoring System, Infopia, South Korea). Animals with fasting blood glucose levels <250 mg/dl were considered

to have diabetes (24).

Experimental design

A total of 40 animals were selected and placed into four groups (n=10 per group). Group 1 was the control group that injected via the tail veins for six weeks. Group 2 (sham group) received 100 µg of an exosome solution in 100 µl of PBS that was injected through the tail veins once per day for six weeks. Group 3 comprised the diabetes group, where rat received a single i.p. injection of STZ (50 mg/kg). Group 4 was the diabetes+KTC-Exos group that received 100 µg of the exosome solution in 100 µl of PBS by injection (25, 26) into the tail veins once per day for six weeks. The animals were separately placed in metabolic cages for 24 hours with access to drinking water in order to measure the 24-hour urine total protein levels upon the completion of the experiment.

Measurement of 24-hour urine protein, blood urea nitrogen and serum creatinine levels

A Bicinchoninic acid (BCA) kit was used to measure urine that was collected following the 6th week of exosome treatment. A combination of the urine and BCA working solution was incubated at 37°C for 30 minutes, and optical density (OD) was examined at a wavelength of 562 nm. At the end of experimental period, the rats were sacrificed after administration of chloral hydrate anaesthesia. Blood plasma was collected from left ventricles of the rats and centrifuged at 3500 rpm for 5 minutes. Both the serum creatinine (Scr) and blood urea nitrogen (BUN) levels were measured by kits (Scr, C011-1, BUN, C013-2, both purchased from Jiangcheng Bio, Nanjing, China). Then, the kidneys were removed. The left kidneys were washed by PBS and fixed with 10% buffered formalin for sectioning into paraffin sections followed by periodic acid-Schiff (PAS) staining. The right kidneys were rinsed, snap-frozen in liquid nitrogen and stored at -80°C for the *miR-29a* and *miR-377* assays.

Light microscopy examination

We observed the PAS stained sections under a light microscope. Summarily, the mesangial area was counted as mesangial expansion, which was determined in 20 consecutive glomeruli from each rat (26). Finally, the relative mesangial expansion was characterised as the fold change from the normal controls.

Extraction of microRNAs and cDNA synthesis

AnmiRNeasy/Plasma kit (Roche, cat. no.: 05080576001, Germany) was used according to the manufacturer's instructions to extract the miRNAs from the frozen specimens. A spectrophotometer at 260 nm and 280 nm wavelengths (NanoDrop Thermo Fisher Scientific, S.N:D015) was utilized to determine the RNA purity and concentration. Subsequently, cDNA was synthesized from 1 µg of total RNA using amiScript II RT Kit (BONmiR, BON209001, Iran) based on the company's instructions.

Quantitative real-time polymerase chain reaction

Quantitative real-time polymerase chain reaction (qRT-PCR) with a light cycler 96 RT-PCR system (Roche Diagnostics, Indianapolis, IN, USA) was used to measure miRNA expressions. Each PCR amplification was performed in duplicate and the resultant volume of 13 μL that consisted of 6.5 μL 2x QuantiTect SYBR Green PCR Master Mix, 1 μL cDNA, 4.5 μL RNAase-free water, and 0.5 μL miRNA-specific forward Primer (miR-29a [ACT GAT TTC TTT TGG TGT] or miR-377 [CGA TCA CAC AAA GGC A]; Bonyakhteh), and 0.5 μL universal reverse primer ([ACT TAT GTT TTT GCC GTT T] Bonyakhteh). The initial activation phase was conducted at 95°C for two minutes to activate the HotStarTaq DNA polymerase and then for 40 cycles at 95°C for 5 seconds and 60°C for 30 seconds. Additionally, the non-template control (H_2O) was regularly in each PCR. RNU87, as the internal control, was used to normalize miRNA expression levels and the fold change was computed with $2^{-\Delta\Delta\text{Ct}}$. Each sample was assayed three times.

Statistical analysis

Statistical analysis was carried out with SPSS 16 software (SPSS Inc., USA). The data were analysed using one-way ANOVA followed by post hoc Least Significant Difference (LSD) test and are presented as mean \pm SD. $P < 0.05$ was considered significant.

Results

Kidney tubular cell phenotype

We observed the KTCs in the cell culture flasks every day after the first day of culture. The morphology and growth of these KTCs were checked by light microscopy to verify an epithelial-like morphology and growth rate. The epithelial-like cells showed high rapid growth and were approximately 95% confluent after 3-4 days (Fig.1).

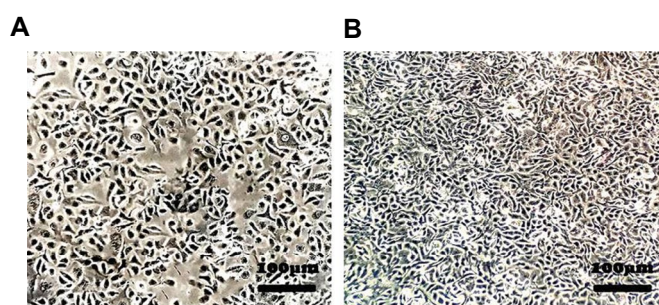


Fig.1: Morphology and growth of kidney tubular cells (KTCs). Growth cells after **A.** Two days and **B.** Four days at $\times 100$ magnification (scale bar: 100 μm).

Transmission electron microscopy evaluation of the exosomes

The exosomes generated by the KTCs were separated from the culture medium by different centrifuge speeds and evaluated by TEM (Fig.2). Ultrastructural analyses of the exosomes showed considerable reinforcement of the typical

spherical-shaped exosomes with diameters of 50-150 nm. In addition, TEM evaluations showed that the exosomes had an average diameter of ≤ 150 nm with an intact round morphology and they possessed membranes (Fig.2A).

Determination of the exosome protein concentration by the Bradford method

The protein concentration of the isolated exosomes was calculated by the Bradford method and BSA was used as the standard. The protein concentration in the sample was 2512 $\mu\text{g}/\text{ml}$.

Scanning electron microscopy evaluation of the exosomes

SEM was used to assess the outer surface characteristics of the exosomes. Small vesicles with round morphology were observed. The size of the vesicles was determined to be 70-260 nm based on the vesicle sizes that were seen in several images. The majority of the vesicles were smaller than 100 nm in size (Fig.2B).

Dynamic light scattering analysis

DLS analysis of the exosomes size showed a bell-shaped size distribution with a peak at about 99.4 nm (Fig.2C).

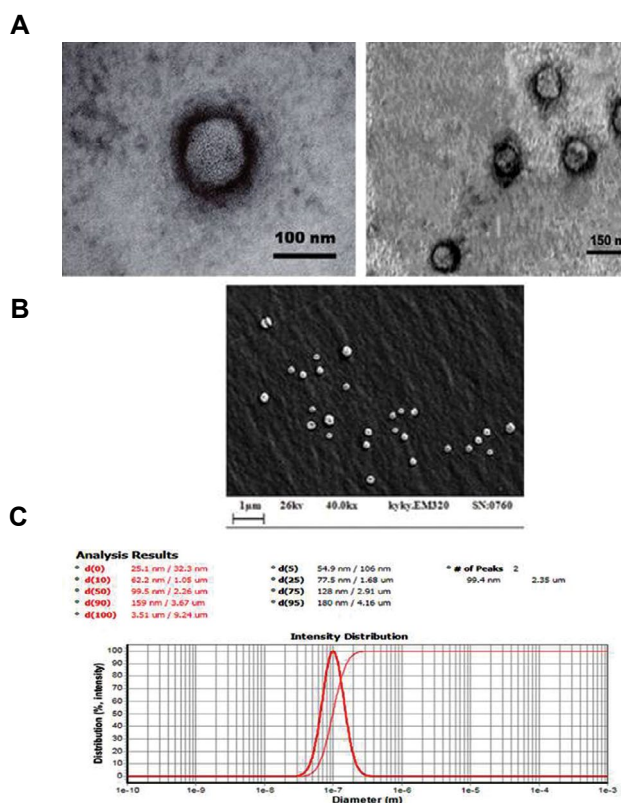


Fig.2: Characterization of exosomes. **A.** Transmission electron microscopy (TEM) observations indicated that the average diameter of the exosomes was ≤ 150 nm. The exosomes had a preserved intact spherical morphology. **B.** Scanning electron microscopy (SEM) analysis showed that the average diameter of the exosomes was ≤ 100 nm and they had a preserved intact spherical morphology. **C.** Dynamic light scattering (DLS) results indicated that almost 50% of the solution ingredients had an average diameter of 99.4 nm.

Western blot analysis

The results of Western blot analysis showed the expressions of two exosome markers, CD63 (25KDa) and CD9 (24-27 KDa), in the KTC-Exos (Fig.3). β -actin (42 KDa) was used as the positive control. Both expression patterns were significant and the results confirmed that the NPs were exosomes.

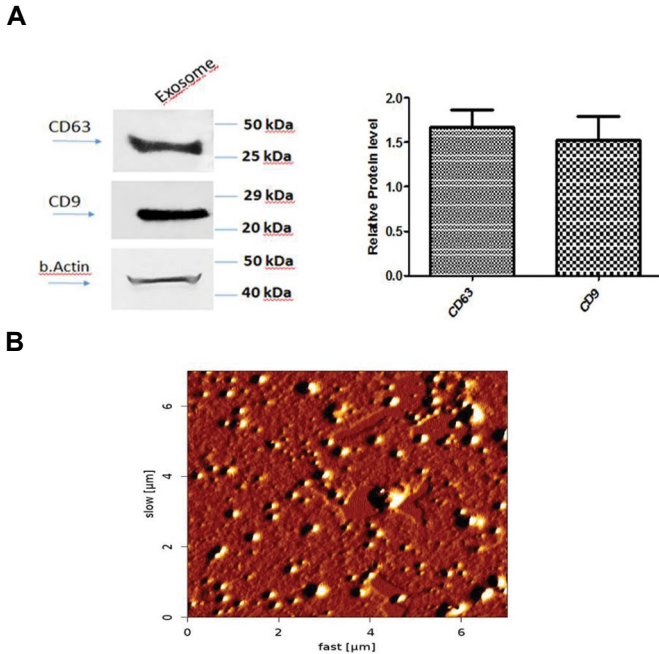


Fig.3: Expression of exosome surface markers by western blotting. **A.** The exosome markers CD9 (24-27 KDa) and CD63 (25 KDa) were expressed in the kidney tubular cell-derived exosomes (KTC-Exos). β -actin (42 KDa) was used as the positive control. **B.** Atomic force microscopy (AFM) image of the KTC-Exos. This showed distinct spherical particles that ranged from 60 to 150 nm.

Atomic force microscopy analysis

AFM obtained from the exosomes showed that the NPs were symmetric, spherical, and without aggregation. The size of the NPs ranged from 60 to 150 nm (Fig.3).

Urine volume in diabetic rats after injection of kidney tubular cell-derived exosomes

Intravenous injection of the KTC-Exos significantly decreased polyuria in the diabetic rats compared with the diabetic group ($P < 0.001$, Fig.4A).

Biochemical analysis

The results showed remarkably elevated Scr, BUN and 24-hour urine protein levels in the diabetic group in comparison to the control group. The KTC-Exos group had significant decreases in Scr ($P < 0.01$), BUN ($P < 0.001$), and 24-hour urine protein ($P < 0.0001$) levels (Fig.4B-D).

Periodic acid-Schiff staining

At the end of the 6th week following the creation of the diabetes model, we observed focal mesangial matrix expansion in the diabetic animals in comparison with the control group (Fig.5A1). Moreover, the section obtained from the diabetic group's kidneys demonstrated partial glomerular hypertrophy and enhanced intra-glomerular cells that were

located mainly in the mesangial region with mesangial expansion (Fig.5BI). In the diabetic animals that received KTC-Exos, there was enhancement in intraglomerular cells and the mesangial matrix. No obvious sign of the rapid growth of the mesangial matrix and glomerular hypertrophy were observed (Fig.5CI). According to quantitative analyses, the KTC-Exos significantly prevented mesangial expansion the mesangial expansion ($P < 0.0001$, Fig.5II).

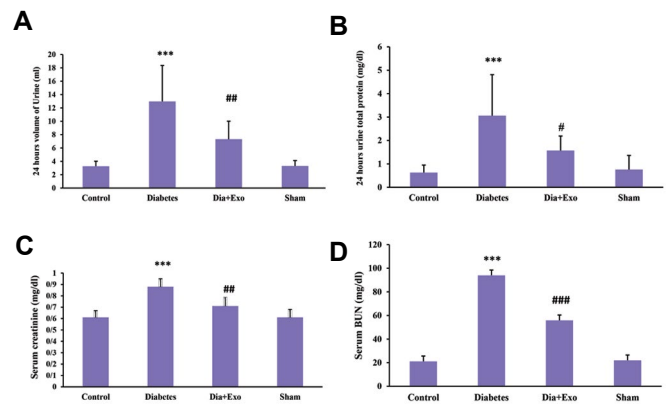


Fig.4: Effects of the kidney tubular cell-derived exosomes (KTC-Exos) on rats with diabetes. **A.** Urine volume, **B.** 24-hour urine protein, **C.** Serum creatinine (Scr), and **D.** Blood urea nitrogen (BUN) levels in the control and diabetes groups before and after treatment with KTC-Exos. Values are expressed as mean \pm SD for eight rats. ***, $P < 0.0001$ (comparison with control), #, $P < 0.01$, ##, $P < 0.001$, and ###, $P < 0.0001$ (comparison with diabetes).

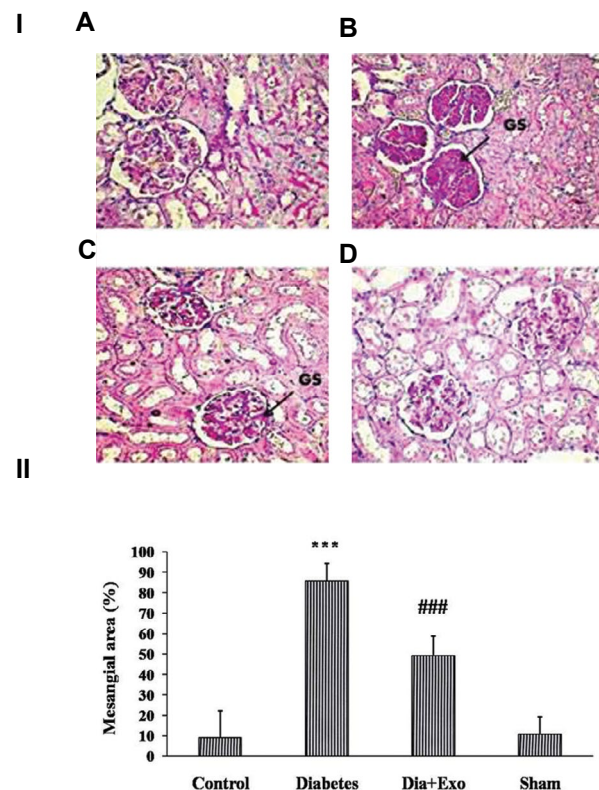


Fig.5: Intravenous injection of the kidney tubular cell-derived exosomes (KTC-Exos) ameliorated the changes in renal histopathology in diabetic rats after six weeks. **1.** Light microscopy examination of tissue sections that were stained by periodic acid-Schiff (PAS) from the different groups. **A.** Control, **B.** Diabetic, **C.** Diabetes treated with KTC-Exos, and **D.** Sham groups. **2.** Quantitative analysis of mean mesangial area from each group of rats. The results are expressed as the means \pm standard deviation for eight rats. ***, $P < 0.0001$, versus control group, ###, $P < 0.0001$, versus diabetic group, and GS; Glomerulosclerosis (magnification: $\times 400$).

Effect of kidney tubular cell-derived exosomes on expression levels of miR-377 and miR-29a

As seen in Figure 6, the qRT-PCR results show that *miR-377* expression considerably increased, whereas *miR-29a* expression significantly decreased following DN. In the KTC-Exos group, the level of increased *miR-377* significantly decreased ($P < 0.001$) and *miR-29a* expression significantly ($P < 0.001$). The levels of *miR-377* and *miR-29a* in the sham group were similar to the control group.

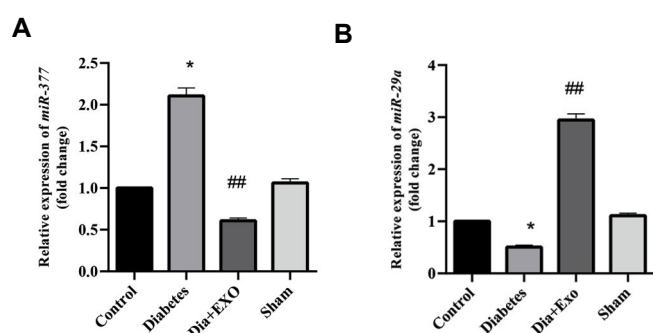


Fig.6: The effect of kidney tubular cell-derived exosomes (KTC-Exos) on the expression levels of **A.** *miR-377* and **B.** *miR-29a* following diabetic nephropathy (DN) injury. The quantitative real-time polymerase chain reaction (qRT-PCR) results showed that *miR-377* expression was significantly increased ($P < 0.01$) whereas *miR-29a* expression significantly decreased ($P < 0.01$) in the DN rats. The expression level of *miR-377* in the Dia+Exo Rats was significantly lower compared to the diabetes group, and the expression level of *miR-29a* in Dia+Exo Rats was significantly higher than the diabetes group. Data are presented as the means \pm standard deviation for eight rats. *, $P < 0.01$ versus the control group and ##, $P < 0.001$ versus the diabetes group.

Discussion

This study was designed to assess exosomes derived from highly differentiated KTCs as treatment for DN. DN is one of the main causes of ESRD and it is characterised by pathological modifications to the kidneys, which results in progressive loss of glomerular filtration rate, tubule-interstitial fibrosis, and proteinuria. Current treatments include precise monitoring of blood pressure and glucose levels, as well as blockage of the rennin-angiotensin mechanism in order to stop DN progression (27). However, novel treatment options for DM should be devised by experts in this field. Notably, several parameters could influence DN expansion after the onset of proteinuria (28).

The present study focused on the main factors involved in DN - endothelial cells and podocytes, both of which have tremendous contributions to the creation of filtration barriers. Increased glucose may decrease density and the numbers of podocytes, eliminate integrity of glomerular filtration membranes, modify its selective permeability, and enhance the development of glomerular sclerosis that can increase DN. Both loss and injury of the interacting proteins of the podocytes can promote apoptosis and destroy slit membrane integrity, thereby aggravating proteinuria and accelerating development of DN (29).

The potential use for exosomes in various research and

clinical practices has made it one of the probable therapeutic options for improving DN. In comparison to stem cells, KTCs also have advantages, especially in regenerative medicine. Some important studies have focused on the effects of exogenous kidney-derived exosomes on renal failure, such as ischemia-reperfusion (30). It is hypothesized that differentiated kidney cells may present more advanced developmental and cell differentiation impacts in comparison with undifferentiated cells; the contents of their exosomes may be different and more effective in treating renal injuries.

We isolated the exosomes by performing sequential and differential centrifugation procedures, as a general strategy, which resulted in the successful generation of KTC-Exos. Next, we assessed the ability of these KTC-Exos to control or reverse DN. The rats that received the KTC-Exos showed significant suppression of polyuria, proteinuria, Scr, and BUN expression levels. One of the main purposes of the present study was to evaluate the impact of KTC-Exos on *miR-29a* and *miR-377* expression in DN progression and pathogenesis in diabetic rats. We observed a considerable increase in mean *miR-377* expression and a significant decrease in mean *miR-29a* expression in the DN animals compared to the control group. This study showed that KTC-Exos administration led to significant downregulation of *miR-377* and upregulation of *miR-29a* in kidney cells of the treated rats. These results suggested that KTC-Exos had a protective function in high glucose-induced miRNA and growth factors (31).

miRNA dysregulations have been identified in many research areas, including DN (32). miRNAs are pivotal regulators of cellular and molecular pathways; therefore, identifying the targets of DN-associated miRNAs can provide further insights into the pathogenesis of DN (33).

In addition, miRNAs in extracellular environments are the essential modulators in renal fibrosis, DN, progressive kidney diseases, and acute kidney injuries. The miRNAs packed in extracellular vesicles, like exosomes, have shown modifications in concentrations related to the incidence of DN and are considered to be potent non-invasive biomarkers that can be used to diagnose and treat DN in patients (34).

There was high expression of *miR-377* in the increased glucose-treated cultured cells, Transforming growth factor beta (*TGF- β*) treated humans, and mice mesangial cells. Increased expression of *miR-377* led to suppression of *p21*-activated kinases and superoxide dismutase, which promoted fibronectin expression. The results of previous studies have shown that *miR-377* caused a decrease in the activities of some target genes, *PAK1* and *SOD1/2*. This led to increased vulnerability to the oxidant stresses and fibronectin accumulation in the extracellular matrix (ECM) (35). Therefore, this miRNA could pivotally contribute to the response of the mesangial cells to diabetic medium and may be a target miRNA for therapy.

Other miRNAs, such as the *miR-29* family (*miR-29a*, *miR-29b*, *miR-29c*), are responsible for anti-fibrotic effects in DN. *miR-29a* directly targets the 3'UTR of *COL4a1* and *COL4a2*, leading to decreased expressions of these two fibrotic genes (36). The *miR-29* family targets a group of mRNAs that encode the proteins implicated in fibrosis, as numerous collagens, elastin and fibrillin. Consequently, decreased *miR-29* expression activates such mRNAs expressions and promotes fibrotic responses (37). In cultured human proximal tubular epithelial cells, increased glucose and *TGF-β1* decrease *miR-29a* expression. Collagen IV is reported to be a target of *miR-29a*, and *miR-29a* regulates collagen expression. Decreased *miR-29a* levels in diabetes may increase collagen deposition, thus mediating the DN pathogenesis (38).

Recent studies have focused on exosomes as treatments for chronic disease models. Exosomes provide protection against the development of chronic kidney damage via suppression of GS, tubulointerstitial fibrosis and capillary rarefaction. For example, researchers examined exosomes with six months following an ischaemia-reperfusion injury (IRI) kidney model and reported that renal microvascular density rarefaction in the presence of sustained hypoxia had a correlation with acceleration of development towards chronic kidney diseases. Microvesicles can reduce tubule-interstitial fibrosis, microvascular rarefaction, and GS, which maintain renal functions (39). Furthermore, the obtained histopathological results showed the ability of exosomes decrease kidney damage, including GS, in a diabetic model.

Based on the literature and the present study results, exosomes extracted from the KTCs may prevent kidney impairments in diabetic patients. Therefore, the combination of exosomes and KTCs would be an encouraging treatment approach in regenerative medicine that would have less immune rejection, increased stability and more acceptable differentiation.

Conclusion

The present findings showed that exosomes derived from KTCs can ameliorate kidney damages in animals with diabetes. Several miRNAs are involved in the pathogenesis and development of DN, where as other miRNAs prevent this disease. Restoration of miRNAs expression to a normal level may be a therapeutic potential for stopping or attenuating disease progression. We have shown that administration of KTC-Exos resulted in upregulation of *miR-377* and downregulation of *miR-29a* in DN, and significantly modulated and improved the symptoms of this disease. These miRNAs present a notable capacity for acting as biomarkers for diagnosing, treating, and prognosis of DN. One of the newly developed treatment approaches would be to apply KTC-Exos for treatment of DN. The effects of exosomes on abnormal regression, damage to podocyte cells, and thickening of the glomerular basement membrane, which are complications of DN, should be taken into consideration in future studies.

Acknowledgments

This manuscript was extracted from the Ph.D. thesis of Fereshtesadat Fakhredini and supported by a grant (CMRC-9805) from the Research Council of Ahvaz Jundishapur University of Medical Sciences in 2019. The authors declare that there are no conflicts of interest.

Authors' Contributions

F.S.F., M.O., E.M.; Contributed to the study conception and design, performed all of the experiments, data and statistical analysis, and interpreted the data. F.S.F., S.A.M., M.R.; Performed western blot and real-time PCR techniques. A.V.G.; Contributed to the cell culture work. M.O., E.M.; Supervised the research. F.S.F.; Drafted the manuscript, which was revised by M.O. and E.M. All authors read and approved the final manuscript.

References

- Martínez-Castelao A, Navarro-González JF, Górriz JL, de Alvaro F. The concept and the epidemiology of diabetic nephropathy have changed in recent years. *J Clin Med*. 2015; 4(6): 1207-1216.
- Saran R, Robinson B, Abbott KC, Agodoa LYC, Albertus P, Ayanian J, et al. US renal data system 2016 annual data report: epidemiology of kidney disease in the United States. *Am J Kidney Dis*. 2017; 69(3Suppl 1): A7-A8.
- Sagoo MK, Gnudi L. Diabetic nephropathy: is there a role for oxidative stress? *Free Radic Biol Med*. 2018; 116: 50-63.
- Cao Q, Chen XM, Huang C, Pollock CA. MicroRNA as novel biomarkers and therapeutic targets in diabetic kidney disease: an update. *FASEB Bioadv*. 2019; 1(6): 375-388.
- Kim MK. Treatment of diabetic kidney disease: current and future targets. *Korean J Intern Med*. 2017; 32(4): 622-630.
- Ahmad J. Management of diabetic nephropathy: recent progress and future perspective. *Diabetes MetabSyndr*. 2015; 9(4): 343-358.
- Nagaishi K, Mizue Y, Chikenji T, Otani M, Nakano M, Konari N, et al. Mesenchymal stem cell therapy ameliorates diabetic nephropathy via the paracrine effect of renal trophic factors including exosomes. *Sci Rep*. 2016; 6: 34842.
- Dominguez JH, Liu Y, Gao H, Dominguez JM 2nd, Xie D, Kelly KJ. Renal tubular cell-derived extracellular vesicles accelerate the recovery of established renal ischemia reperfusion injury. *J Am Soc Nephrol*. 2017; 28(12): 3533-3544.
- Roy S, Hochberg FH, Jones PS. Extracellular vesicles: the growth as diagnostics and therapeutics; a survey. *J Extracell Vesicles*. 2018; 7(1): 1438720.
- Li JS, Li B. Renal injury repair: how about the role of stem cells. *Adv Exp Med Biol*. 2019; 1165: 661-670.
- Wang SY, Hong Q, Zhang CY, Yang YJ, Cai GY, Chen XM. miRNAs in stem cell-derived extracellular vesicles for acute kidney injury treatment: comprehensive review of preclinical studies. *Stem Cell Res Ther*. 2019; 10(1): 281.
- Keshkar S, Azarpira N, Ghahremani MH. Mesenchymal stem cell-derived extracellular vesicles: novel frontiers in regenerative medicine. *Stem Cell Res Ther*. 2018; 9(1): 63.
- Kato M. Noncoding RNAs as therapeutic targets in early stage diabetic kidney disease. *Kidney Res Clin Pract*. 2018; 37(3): 197-209.
- Yang H, Lian D, Zhang X, Li H, Xin G. Key genes and signaling pathways contribute to the pathogenesis of diabetic nephropathy. *Iran J Kidney Dis*. 2019; 13(2): 87-97.
- Ma N, Xiang Y, Zhang Y, Zhao X, Zhou L, Gao X. The balance mediated by miRNAs and the hemeoxygenase 1 feedback loop contributes to biological effects. *J Cell Biochem*. 2013; 114(12): 2637-2642.
- Li H, Zhang L, Wang F, Shi Y, Ren Y, Liu Q, et al. Attenuation of glomerular injury in diabetic mice with tert-butylhydroquinone through nuclear factor erythroid 2-related factor 2-dependent antioxidant gene activation. *Am J Nephrol*. 2011; 33(4): 289-297.
- Tung CW, Ho C, Hsu YC, Huang SC, Shih YH, Lin CL. MicroRNA-29a Attenuates diabetic glomerular injury through modulating cannabinoid receptor 1 signaling. *Molecules*. 2019; 24(2): 264.

18. Ebadi Z, Moradi N, Kazemi Fard T, Balochnejadmojarrad T, Chamani E, Fadaei R, et al. Captopril and spironolactone can attenuate diabetic nephropathy in wistar rats by targeting microRNA-192 and microRNA-29a/b/c. *DNA Cell Biol.* 2019; 38(10): 1134-1142.
19. Kelly KJ, Zhang J, Han L, Kamocka M, Miller C, Gattone VH 2nd, et al. Improved structure and function in autosomal recessive polycystic rat kidneys with renal tubular cell therapy. *PLoS One.* 2015; 10(7): e0131677.
20. Bär C, Thum T, de Gonzalo-Calvo D. Circulating miRNAs as mediators in cell-to-cell communication. *Epigenomics.* 2019; 11(2): 111-113.
21. Wu R, Huang C, Wu Q, Jia X, Liu M, Xue Z, et al. Exosomes secreted by urine-derived stem cells improve stress urinary incontinence by promoting repair of pubococcygeus muscle injury in rats. *Stem Cell Res Ther.* 2019; 10(1): 80.
22. Nojehdehi Sh, Hashemi SM, Hesampour A. Isolation and characterization of exosomes separated from stem cells by ultra-centrifuge method. *Research in Medicine.* 2018; 41(4): 422-405.
23. Mao F, Wu Y, Tang X, Kang J, Zhang B, Yan Y, et al. Exosomes derived from human umbilical cord mesenchymal stem cells relieve inflammatory bowel disease in mice. *Biomed Res Int.* 2017; 2017: 5356760.
24. Jelodar Gh, Mohammadi M, Akbari A, Nazifi S. Cyclohexane extract of walnut leaves improves indices of oxidative stress, total homocysteine and lipids profiles in streptozotocin-induced diabetic rats. *Physiol Rep.* 2020; 8(1): e14348.
25. Ebrahim N, Ahmed IA, Hussien NI, Dessouky AA, Farid AS, Elshazly AM, et al. Mesenchymal stem cell-derived exosomes ameliorated diabetic nephropathy by autophagy induction through the mTOR signaling pathway. *Cells.* 2018; 7(12): 226.
26. Jiang ZZ, Liu YM, Niu X, Yin JY, Hu B, Guo SC, et al. Exosomes secreted by human urine-derived stem cells could prevent kidney complications from type I diabetes in rats. *Stem Cell Res Ther.* 2016; 7: 24.
27. Sun ZJ, Li XQ, Chang DY, Wang SX, Liu G, Chen M, et al. Complement deposition on renal histopathology of patients with diabetic nephropathy. *Diabetes Metab.* 2019; 45(4): 363-368.
28. Shi JX, Huang Q. Glucagon-like peptide-1 protects mouse podocytes against high glucose-induced apoptosis, and suppresses reactive oxygen species production and proinflammatory cytokine secretion, through sirtuin 1 activation in vitro. *Mol Med Rep.* 2018; 18(2): 1789-1797.
29. Zhan X, Yan C, Chen Y, Wei X, Xiao J, Deng L, et al. Celastrol antagonizes high glucose-evoked podocyte injury, inflammation and insulin resistance by restoring the HO-1-mediated autophagy pathway. *Mol Immunol.* 2018; 104: 61-68.
30. Dominguez JH, Liu Y, Gao H, Dominguez JM, Xie D, Kelly KJ. Renal Tubular cell-derived extracellular vesicles accelerate the recovery of established renal ischemia reperfusion injury. *J Am Soc Nephrol.* 2017; 28(12): 3533-3544.
31. Nargesi AA, Lerman LO, Eirin A. Mesenchymal stem cell-derived extracellular vesicles for renal repair. *Curr Gene Ther.* 2017; 17(1): 29-42.
32. Fan B, Luk AOY, Chan JCN, Ma RCW. MicroRNA and diabetic complications: a clinical perspective. *Antioxid Redox Signal.* 2018; 29(11): 1041-1063.
33. Simpson K, Wonnacott A, Fraser DJ, and Bowen T. MicroRNAs in diabetic nephropathy: from biomarkers to therapy. *Curr Diab Rep.* 2016; 16(3): 35.
34. Petrillo F, Iervolino A, Zacchia M, Simeoni A, Masella C, Capolongo G, et al. MicroRNAs in Renal diseases: a potential novel therapeutic target. *Kidney Dis (Basel).* 2017; 3(3): 111-119.
35. Al-Kafaji G, Al-Muhtareh HA. Expression of microRNA-377 and microRNA-192 and their potential as blood-based biomarkers for early detection of type 2 diabetic nephropathy. *Mol Med Rep.* 2018; 18(1): 1171-1180.
36. Wang B, Wang J, He W, Zhao Y, Zhang A, Liu Y, et al. Exogenous miR-29a attenuates muscle atrophy and kidney fibrosis in unilateral ureteral obstruction mice. *Hum Gene Ther.* 2020; 31(5-6): 367-375.
37. Wang B, Komers R, Carew R, Winbanks CE, Xu B, Herman-Edelstein M, et al. Suppression of microRNA-29 expression by TGF- β 1 promotes collagen expression and renal fibrosis. *J Am Soc Nephrol.* 2012; 23(2): 252-265.
38. Du B, Ma LM, Huang MB, Zhou H, Huang HL, Shao P, et al. High glucose down-regulates miR-29a to increase collagen IV production in HK-2 cells. *FEBS Lett.* 2010; 584(4): 811-816.
39. Meng W, He C, Hao Y, Wang L, Li L, Zhu G. Prospects and challenges of extracellular vesicle-based drug delivery system: considering cell source. *Drug Deliv.* 2020; 27(1): 585-598.